

# Signaling Pathways Regulating Intercellular Adhesion Molecule 1 Expression by Endothelin 1

## Comparison With Interleukin-1 $\beta$ in Normal and Scleroderma Dermal Fibroblasts

Charlotte E. Waters,<sup>1</sup> Xu Shi-Wen,<sup>2</sup> Chris P. Denton,<sup>2</sup> David J. Abraham,<sup>2</sup> and Jeremy D. Pearson<sup>1</sup>

**Objective.** Endothelin 1 (ET-1) has been implicated in the pathogenesis of fibrotic and inflammatory diseases, including scleroderma. In addition to modulating vascular tone and extracellular matrix turnover, ET-1 up-regulates cell surface adhesion molecules including intercellular adhesion molecule 1 (ICAM-1), which is key to cell–cell and cell–matrix adhesion and leukocyte infiltration. This study was undertaken to delineate the signal transduction pathways utilized by ET-1 and compare them with those adopted by proinflammatory cytokine interleukin-1 $\beta$  (IL-1 $\beta$ ) in normal and scleroderma dermal fibroblasts.

**Methods.** Protein expression induced by ET-1 and IL-1 $\beta$  on normal dermal fibroblasts, with or without signaling inhibitors, was detected by enzyme-linked immunosorbent assay, while messenger RNA (mRNA) levels were analyzed by LightCycler polymerase chain reaction. Expression of protein kinase C $\delta$  (PKC $\delta$ ) and PKC $\epsilon$  protein in normal dermal fibroblasts and scleroderma dermal fibroblasts was determined by Western blotting, and PKC $\epsilon$  involvement in ET-1 signaling was confirmed through transfection of an ICAM-1 promoter construct into murine PKC $\epsilon$ <sup>-/-</sup> fibroblasts. NF- $\kappa$ B activation was confirmed via electrophoretic mobility

supershift assay, and analysis of the ICAM-1 promoter region was achieved via transfection of deletion constructs into human dermal fibroblasts.

**Results.** In normal dermal fibroblasts, ET-1 induced ICAM-1 mRNA and surface protein expression in a dose- and time-dependent manner via both receptor subtypes, ET<sub>A</sub> and ET<sub>B</sub>; antagonism of both abolished the ET-1 response. MEK was involved in the signaling cascade, but phosphatidylinositol 3-kinase and p38 MAPK were not. Key to the cascade was activation of NF- $\kappa$ B, achieved by ligation of either receptor subtype. PKC $\epsilon$  activation led to downstream activation of MEK and, in part, NF- $\kappa$ B. IL-1 $\beta$  signaling required NF- $\kappa$ B and MEK activation, along with activation of PKC $\delta$ . ET-1 and IL-1 $\beta$  each utilized the same ICAM-1 promoter region and the same NF- $\kappa$ B site at -157 bp. Responses to ET-1 and IL-1 $\beta$  differed in scleroderma dermal fibroblasts, with ET-1 sensitivity decreasing and IL-1 $\beta$  responses remaining intact. Expression of PKC $\epsilon$  and PKC $\delta$  in scleroderma dermal fibroblasts was also altered.

**Conclusion.** The findings of this study indicate that differences in sensitivity to ET-1 and IL-1 $\beta$  in scleroderma dermal fibroblasts may be explained by altered expression of the PKC isoforms and cytokine receptors.

Since its identification in 1988, the peptide mediator endothelin-1 (ET-1) has been shown to act as a potent modulator of vascular tone, extracellular matrix turnover, and cell proliferation (1–3). There is now strong evidence that ET-1 additionally plays a key role in fibrosis, not only as part of the physiologic wound healing response, but also in pathology (4). ET-1 is

Supported by the Wellcome Trust, the Arthritis Research Campaign, and the Raynaud's and Scleroderma Association.

<sup>1</sup>Charlotte E. Waters, PhD, Jeremy D. Pearson, PhD: King's College London, London, UK; <sup>2</sup>Xu Shi-Wen, PhD, Chris P. Denton, MB, PhD, David J. Abraham, PhD: Royal Free and University College Medical School, London, UK.

Address correspondence and reprint requests to Jeremy D. Pearson, MD, Cardiovascular Division, 2.32B New Hunt's House, School of Biomedical Sciences, Guy's Campus, King's College London, London SE1 1UL, UK. E-mail: jeremy.pearson@kcl.ac.uk.

Submitted for publication July 8, 2005; accepted in revised form October 25, 2005.

proinflammatory, priming neutrophils, activating mast cells, and stimulating cytokine production from monocytes (5–7). In addition, it up-regulates the expression of intercellular adhesion molecule-1 (ICAM-1) on a variety of cell types (8). This is of potential importance in diseases such as pulmonary hypertension and the connective tissue disease scleroderma (systemic sclerosis; SSc), where ET-1 has been implicated in pathogenesis and ICAM-1 plays a role in cell–cell and cell–matrix adhesion and leukocyte infiltration. In SSc, ICAM-1 expression is elevated in blood vessels and fibroblasts, and in the circulation as a soluble factor (9,10). However, the mechanism by which ET-1 regulates ICAM-1 has not been defined.

ET-1 acts at either of 2 G protein–coupled receptors (ET<sub>A</sub> and ET<sub>B</sub>), each classically linked to elevation of cytosolic Ca<sup>2+</sup> levels (11). Both ET<sub>A</sub> and ET<sub>B</sub> receptors are present and functional in human dermal fibroblasts, at ~4,000 and ~600 surface receptors per cell, respectively (2). Activated ET receptors can recruit more than one type of G $\alpha$  subunit, with consequent selectivity in downstream signaling. However, there is considerable overlap in signaling induced by ET<sub>A</sub> and ET<sub>B</sub> receptors, and there is recent evidence of receptor heterodimer formation (12). In specific cell types, elevation of Ca<sup>2+</sup> and/or activation of protein kinase C (PKC), PKA, phosphatidylinositol 3-kinase (PI 3-kinase), and MAPK have been reported (12–15).

ICAM-1 is a member of the immunoglobulin gene superfamily and expressed constitutively by many cell types. Expression of the protein can be up-regulated severalfold by cytokines such as interferon- $\gamma$ , interleukin-1 $\beta$  (IL-1 $\beta$ ), and tumor necrosis factor  $\alpha$ , as well as other signaling factors or activating stimuli such as lipopolysaccharide, the PKC-activating phorbol ester phorbol myristate acetate, and hydrogen peroxide (16–18). Intracellular signaling pathways implicated in the regulation of ICAM-1 expression in response to these stimuli include PKC, MAPK (ERK, p38, and JNK), and NF- $\kappa$ B (for review, see ref. 19), with the most important transcription factors being activator protein 1 (AP-1), NF- $\kappa$ B, Ets, CCAAT/enhancer binding protein (c/EBP), signal transducer and activator of transcription, and SP-1 (17,19). The signaling pathways activated depend on the agonist, may differ between cell types, and have not previously been studied using ET-1.

The primary purpose of this study was to delineate the signaling cascades activated by ET-1 in mediating ICAM-1 expression in normal dermal fibroblasts. After identifying these cascades, we compared them with those adopted by IL-1 $\beta$ . We found that the predominant

signaling pathways leading to increased fibroblast ICAM-1 expression in response to ET-1 are equivalently activated by either ET<sub>A</sub> or ET<sub>B</sub> receptors, targeting NF- $\kappa$ B binding to the proximal ICAM-1 promoter site, which is also required for IL-1 $\beta$ –induced ICAM-1 expression. The signal transduction pathways of ET-1 and IL-1 $\beta$  each involve activation of MEK. However, ET-1 signaling requires activation of PKC $\epsilon$ , while activation of PKC $\delta$  appears important in IL-1 $\beta$ –driven responses. Finally, we demonstrated altered expression of these PKC isoforms in scleroderma dermal fibroblasts, which may contribute to the changes in ICAM-1 gene responsiveness to these cytokines.

## MATERIALS AND METHODS

**Cell culture.** Human dermal fibroblasts at passage 5 were obtained from American Type Culture Collection (Rockville, MD) and cultured in Dulbecco's modified Eagle's medium (DMEM) with L-glutamine and 10% fetal bovine serum (FBS) (Sigma, Poole, UK). Cells were incubated at 37°C, 5% CO<sub>2</sub> in a humid atmosphere, and not used after passage 25.

In studies involving comparisons between SSc patients and controls, cells were obtained via punch biopsy (4 mm<sup>3</sup>) from the forearm of healthy individuals and clinically involved skin of patients with diffuse cutaneous SSc. All patients in the study were diagnosed as having diffuse scleroderma using the classification established by LeRoy et al (20). The healthy controls were closely matched for age and sex. The mean age of the patients was 38 years (range 29–45). Fibroblasts were obtained from the biopsy samples by *in vitro* culture as previously described (21). In experiments, normal and scleroderma fibroblasts were used at identical passage (between passages 3 and 5). To reduce any potential influence on the data of differing growth rates of the cells, and also the mitogenic effect of ET-1 (3), experiments involving normal dermal fibroblasts and scleroderma dermal fibroblasts were performed on cells at >90% confluence. Fibroblasts from wild-type mice and PKC $\epsilon$ -knockout animals were generated, genotyped, and cultured as previously described (22).

**Cellular enzyme-linked immunosorbent assay (ELISA).** *Culture of cells for ET-1 dose-response and time course studies.* Human dermal fibroblasts were seeded into 96-well plates at a density of  $5 \times 10^3$  cells per well. After culture for 48 hours in DMEM/10% FBS, the medium was replaced with serum-free (0.5% bovine serum albumin) DMEM, and ET-1 was added. Experiments were performed over a 48-hour period (dose-response studies) or a 24-hour period (time course studies), under serum-free conditions. Replicate wells (3–6 wells) were used for each test condition in at least 3 independent experiments using different fibroblast cultures.

*Culture of cells for inhibitor studies.* Human dermal fibroblasts were seeded into 96-well plates at a density of  $5 \times 10^4$  cells per well. After culture for 24 hours, cells were pretreated with inhibitor or receptor antagonist (when appropriate) for 1 hour prior to 24-hour stimulation with 100 nM ET-1 (Bachem, Merseyside UK) or 10 ng/ml IL-1 $\beta$  (R&D Systems, Abingdon, UK). Inhibitors used were PG490 (Trip-

tolide; 100 nM), bisindolylmaleimide I (100–500 nM), SB203580 (5  $\mu$ M), and wortmannin (50 nM) (all from Calbiochem, Abingdon, UK) JKC-301 and BQ-788 (both 10  $\mu$ M; Bachem) U0126 (10  $\mu$ M; Sigma), and bosentan (10  $\mu$ M; Actelion, Allschwil, Switzerland). Inhibitors were used at doses calculated to achieve complete inhibition based on their 50% inhibition concentration (IC<sub>50</sub>) values, while antagonists were used at supramaximal doses for complete antagonism. Experiments were performed in DMEM/10% FBS, with replicate wells used for every condition in at least 3 independent experiments using different fibroblast cultures.

**ICAM-1 ELISA.** ICAM-1 expression was measured using a cell-bound ELISA. Briefly, cells were washed with phosphate buffered saline (PBS) and fixed in 0.1% glutaraldehyde solution for 10 minutes at 4°C. Nonspecific antibody binding was blocked using PBS/5% fat-free milk for 1 hour. Cells were incubated with primary antibody (0.5  $\mu$ g/ml) for 1 hour in PBS/5% milk. Primary antibodies included negative controls of mouse IgG (Dako, Cambridge, UK), irrelevant antibody (rat anti-mouse ICAM-1; R&D Systems), and a positive control of anti-human HLA class I antigen (Dako), alongside mouse anti-human ICAM-1 (Dako). After washing, cells were further incubated with rabbit anti-mouse secondary antibody at a 1:2,000 dilution (Sigma) in PBS/5% milk. After further washes with PBS/5% milk followed by PBS alone, antibody binding was determined using *o*-phenylenediamine/H<sub>2</sub>O<sub>2</sub> solution (Sigma-Fast OPD tablets; Sigma) and measurement of absorbance at 450 nm. Surface ICAM-1 expression as determined by ELISA was defined based on 100% being the maximal increase in ligand-induced expression over basal levels.

**Reverse transcription–polymerase chain reaction (PCR).** Cells were stimulated with or without ET-1 (100 nM) or IL-1 $\beta$  (10 ng/ml) for 0, 1, 2, 4, 6, or 24 hours in serum-containing medium. When appropriate, cells were preincubated with NF- $\kappa$ B inhibitor PG490 (100 nM), MEK inhibitor PD98059 (40  $\mu$ M), or PKC $\delta$ -specific inhibitor Rottlerin (6  $\mu$ M) 1 hour prior to the addition of agonist. Total RNA was isolated using TRIzol reagent (Invitrogen, Paisley, UK) and precipitated using isopropanol and 75% ethanol. RNA was quantitated using spectrometry, and integrity verified by gel electrophoresis. Total RNA (0.5  $\mu$ g) was reverse transcribed in a 20- $\mu$ l reaction volume containing both oligonucleotide dT (dT<sub>18</sub>) and random decamers (dN<sub>10</sub>), using Moloney murine leukemia virus reverse transcriptase (Promega, Southampton, UK), for 1 hour at 37°C. The complementary DNA was diluted to 100  $\mu$ l with diethylpyrocarbonate-treated water and the target measured by real-time quantitative PCR with SYBR Green according to the instructions of the manufacturer (Qiagen, Crawley, UK). Triplicate samples were run, transcripts were measured in picograms, and expression values were standardized to values obtained with control 28S ribosomal RNA primers. Primers (Operon, Newcastle, UK) were as follows: 28S as previously described (23), and ICAM-1 5'-GGGAGCTTCGTGTCCTGTATGGCC-3' (forward), 5'-AGTCTGTATTTCTTGATCTTCCGCTGGC-3' (reverse).

**Electrophoretic mobility supershift assay (EMSA).** Protein lysates were prepared from cells cultured in the presence of serum and treated with ET-1 (100 nM) for 0, 30, or 60 minutes. Cells were lysed in cytosolic buffer (10 mM

HEPES, 10 mM KCl, 0.1 mM EDTA, 0.1 mM EGTA, 2 mM dithiothreitol [DTT]) containing protease inhibitors and incubated on ice for 15 minutes. Nonidet P40 (NP40) was added to a final concentration of 1%, and the lysates were vortexed thoroughly and centrifuged at  $\geq 10,000g$  for 30 seconds. The supernatant was removed and stored as the cytosolic protein fraction. The pellet was resuspended in nuclear buffer (10 mM HEPES, 10 mM KCl, 0.1 mM EDTA, 0.1 mM EGTA, 2 mM DTT, 400 mM NaCl, 1% NP40) also containing protease inhibitors, and incubated at 4°C on a rotor mixer for 15 minutes followed by centrifugation at  $\geq 10,000g$  for 5 minutes at 4°C. The resulting supernatant contained the nuclear protein fraction, which was stored at  $-80^\circ\text{C}$  until use. Bradford's protein assay (Bio-Rad, Hertfordshire, UK) was used for quantification.

The NF- $\kappa$ B consensus oligonucleotide (Promega) was  $\gamma$ -<sup>32</sup>P end-labeled and purified using MicroSpin G-25 Sephadex columns (Amersham, Little Chalfont, UK). Protein lysates (5  $\mu$ g) were incubated with 1  $\mu$ l of cold noncompetitive oligonucleotide (Oct-1). Control samples were incubated with a further 1  $\mu$ l of Oct-1 oligonucleotide or 1  $\mu$ l of cold competitive oligonucleotide. In supershift samples, lysates were incubated on ice for 30 minutes with 1  $\mu$ l (2  $\mu$ g) of antibody (anti-p65 [sc-7151X], anti-RelB [sc-266X], or anti-p50 [sc-1190X]; all from Santa Cruz Biotechnology, Santa Cruz, CA) prior to the addition of cold oligonucleotide. All samples were incubated with cold oligonucleotide on ice for 1 hour, followed by the addition of radioactive oligonucleotide and a further incubation of 45 minutes. Complexes were resolved on a 4.5% nondenaturing acrylamide gel using 0.5 $\times$  Tris–borate–EDTA buffer, and the gels were dried and visualized by autoradiography.

**Manufacture of ICAM-1 promoter construct.** A 1.2-kb portion of the ICAM-1 promoter was extracted from an ICAM-pSM construct kindly donated by Dr. S. Martinotti (University of L'Aquila, L'Aquila, Italy) (24), using *Bgl* II (Promega). The isolated fragment was then digested with *Bse* RI, *Avr* II, *Dra* II, *Hind* III, or *Eae* I (all from New England Biolabs, Beverly, MA). Reactions were resolved by gel electrophoresis, and products of the appropriate size were isolated (750, 525, 475, 265, and 157 bp, respectively). The basic luciferase vector, pGL3-LUC (Promega) was linearized in the multiple cloning region using *Nhe* I (New England Biolabs). Both linearized vector and isolated fragment were blunt-ended using *Klenow*, followed by ligation using T4 DNA ligase (both from Promega). Ligation reactions were transformed into DH5 $\alpha$  *Escherichia coli* (Invitrogen). Colony PCR was used to establish inclusion of the insert using the TaqMaster Mix kit (Qiagen) (forward primer [in vector] 5'-CTAACATACGCTCTCCATC-3', reverse primer [in insert] 5'-GTGATCCTTTATAGCGC-3'). Sequencing analysis established the direction of insertion and verified that the correct promoter fragment had been used. All construct nomenclature described in this study is based on the size of the promoter fragment from the TATAA box.

**Transfection.** Fibroblasts were plated into 96-well plates the day before transfection, to achieve 75% confluence. Cells were transfected with 200 ng of ICAM-1 plasmid using jetPEI according to the instructions of the manufacturer (QBiogene, Cambridge, UK). After a 3-hour incubation, cells were washed with sterile PBS, new medium applied, and ET-1

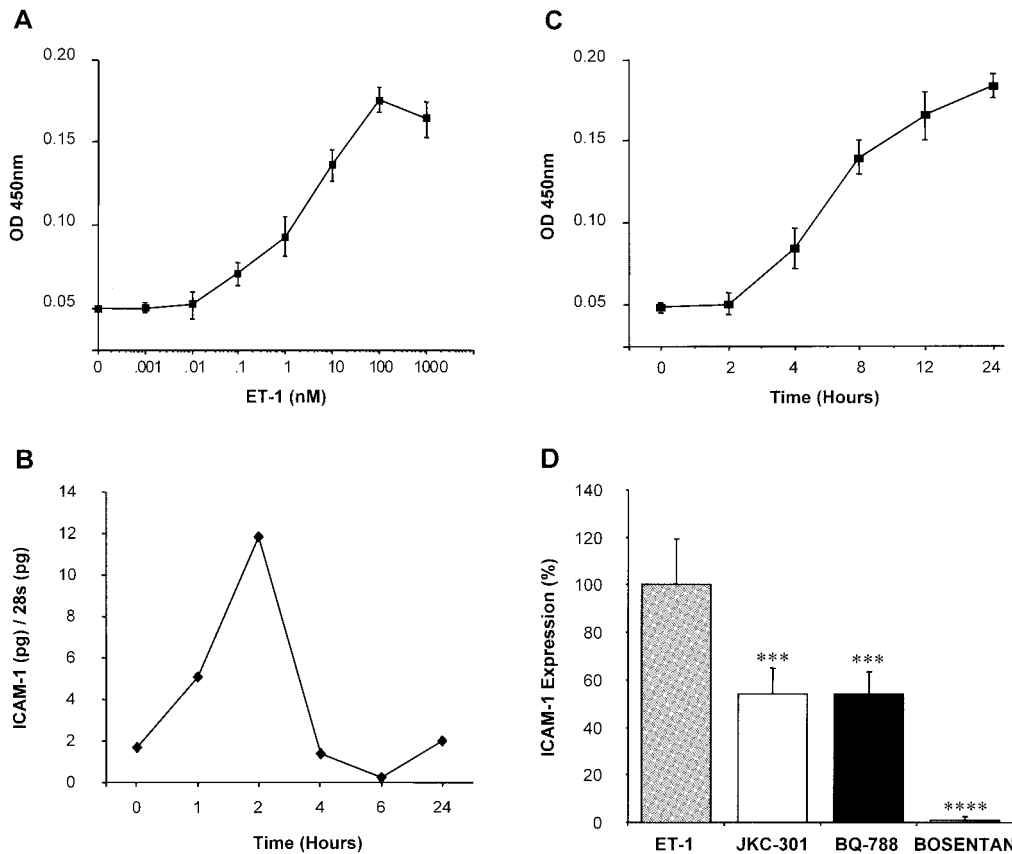


**Figure 1.** Up-regulation of intercellular adhesion molecule 1 (ICAM-1) expression by endothelin 1 (ET-1) via either receptor subtype. Fibroblasts cultured under standard conditions in monolayer cultures expressed low levels of ICAM-1. Stimulation with ET-1 for 48 hours led to a dose-dependent increase in ICAM-1 protein expression (A). Exposure to ET-1 also led to time-dependent increases in levels of ICAM-1 mRNA (B) and protein (C). Fibroblasts pretreated with the  $ET_A$  receptor antagonist JKC-301 (10  $\mu M$ ), the  $ET_B$  receptor antagonist BQ-788 (10  $\mu M$ ), or the dual antagonist bosentan (10  $\mu M$ ) for 1 hour prior to addition of ET-1 expressed lower levels of ICAM-1 than fibroblasts cultured for 24 hours with ET-1 (100 nM) alone (\*\*\* =  $P < 0.001$ ; \*\*\*\* =  $P < 0.0001$ , versus treatment with ET-1 alone) (D). Values are the mean  $\pm$  SD results ( $n = 3$  experiments) obtained by enzyme-linked immunosorbent assay (A, C, and D) or real-time polymerase chain reaction (B). OD 450 nm = optical density at 405 nm.

(100 nM) or IL-1 $\beta$  (10 ng/ml) was added for a further 24 hours. Cell extracts were analyzed for luciferase activity using the Dual-Glo Luciferase Reporter Assay System (Promega). Transfection efficiency was assessed by cotransfection with 50 ng of a plasmid containing the cytomegalovirus promoter linked to a renilla luciferase reporter gene. Transfections were performed on 4 separate occasions, with 5 wells per condition per transfection. Data were normalized using the renilla luciferase readings, and presented as mean  $\pm$  SEM luciferase units.

**Western blotting analysis.** Scleroderma and age-matched normal dermal fibroblasts were cultured in DMEM/10% FBS until 90% confluent. Whole cell lysates of untreated cells were produced by harvesting via scraping with cold RIPA buffer (50 mM Tris base [pH 7.4], 150 mM NaCl, 1% NP40, 0.25% sodium deoxycholate, 1 mM EDTA) containing protease inhibitors (protease inhibitor cocktail; Sigma), and quan-

tification was achieved using Bradford's protein assay. Protein lysate (30  $\mu g$ ) was resolved by sodium dodecyl sulfate-10% polyacrylamide gel electrophoresis, with transfer to polyvinylidene difluoride membrane (MilliQ; Sigma). Nonspecific binding was blocked with Tris buffered saline-Tween (TBST)/5% milk, and the membrane was incubated with primary antibody (rabbit polyclonal anti-human PKC $\epsilon$  [sc-214; Santa Cruz Biotechnology] or PKC $\delta$  [sc-213]) for 1–16 hours. Membranes were washed with TBST prior to incubation for 45 minutes with appropriate secondary antibody in TBST/5% milk. Antibody binding was visualized using enhanced chemiluminescence (Amersham).

**Statistical analysis.** Statistical analysis was carried out by analysis of variance, with posttesting using the Tukey-Kramer multiple comparisons test.  $P$  values less than 0.05 were considered significant.

**RESULTS**

Up-regulation of ICAM-1 expression by ET-1 via either receptor subtype. Consistent with previous reports, we found that ICAM-1 was constitutively expressed on dermal fibroblasts, and expression was enhanced following treatment with ET-1 (Figure 1). Up-regulation of ICAM-1 by ET-1 was concentration dependent, with maximal induction reached at 100 nM (Figure 1A). The time course of ET-1-induced ICAM-1 expression in normal fibroblasts was consistent with up-regulation at a transcrip-

tional level, since quantitation of ICAM-1 messenger RNA (mRNA) production using quantitative PCR (Figure 1B) showed an increase 1 hour after ET-1 stimulation, with a corresponding increase in protein expression apparent from 4 hours after addition of ET-1 (100 nM) (Figure 1C). This indicates that stimulation of these cells with ET-1 has a direct effect on the ICAM-1 promoter. The role of the endothelin receptor subtypes, ET<sub>A</sub> and ET<sub>B</sub>, in the signaling cascade was investigated using the specific antagonists JKC-301 (ET<sub>A</sub>) and BQ-788 (ET<sub>B</sub>) as well as the dual

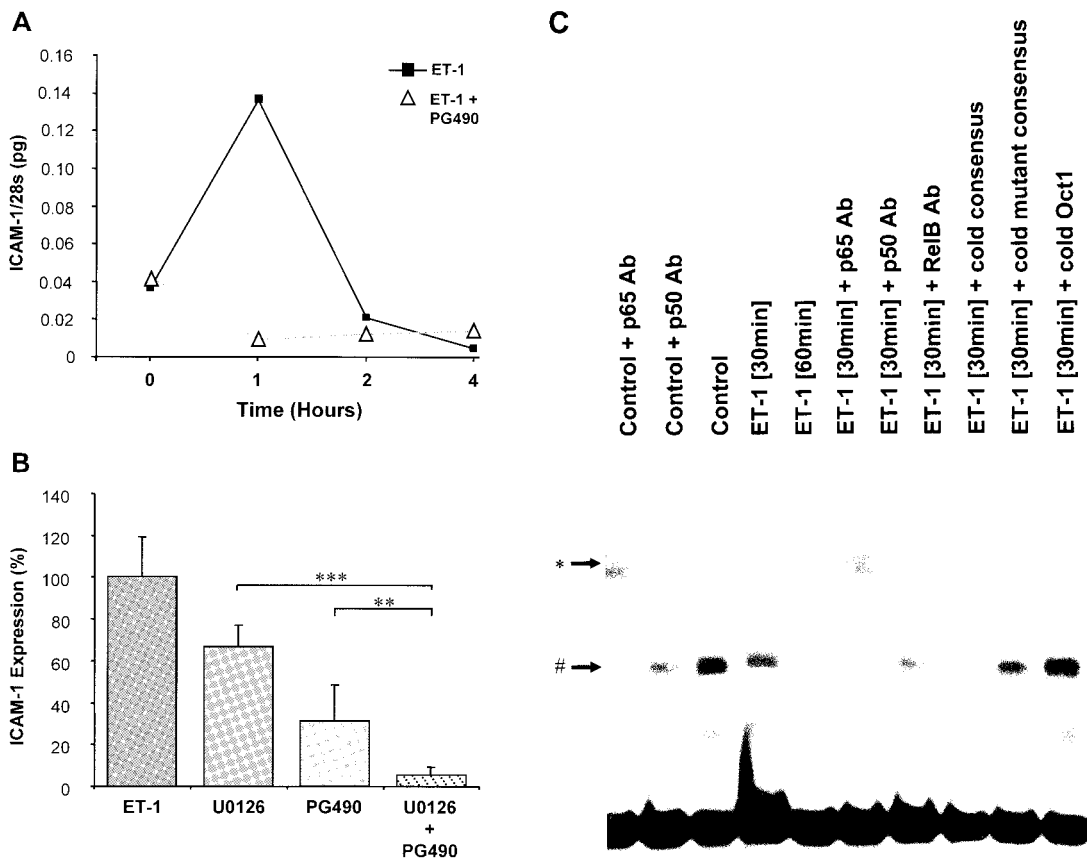


**Figure 2.** Requirement of NF- $\kappa$ B and MEK activation for ET-1-mediated ICAM-1 expression. **A**, Fibroblasts were pretreated with the NF- $\kappa$ B inhibitor PG490 (100 nM) prior to exposure to ET-1 (100 nM). Messenger RNA isolated from the samples, normalized against 28S ribosomal RNA, was used in real-time polymerase chain reaction studies for ICAM-1, performed in triplicate. Values are the mean. **B**, Fibroblasts were cultured in the presence or absence of ET-1 (100 nM) for 24 hours. In some of the experiments, cells were pretreated for 1 hour with PG490, the MEK inhibitor U0126 (10  $\mu$ M), or both. Each inhibitor significantly reduced ET-1-induced ICAM-1 expression, with U0126 and PG490 in combination virtually abolishing the response. \*\* =  $P < 0.01$ ; \*\*\* =  $P < 0.001$ . Values are the percent ICAM-1 expression versus that with ET-1 stimulation alone (mean and SD of 9 experiments). **C**, Electrophoretic mobility supershift assay. Cells were left untreated or were exposed to ET-1 (100 nM) for 30 or 60 minutes. Nuclear fractions were incubated with <sup>32</sup>P-labeled consensus NF- $\kappa$ B oligonucleotide for 45 minutes before resolution on a 4.5% nondenaturing acrylamide gel. Gels were dried, followed by exposure to film. The presence of p65 and p50 subunits in the DNA-bound complex was confirmed by incubating samples with either anti-p65 or anti-p50 antibodies (Ab) prior to incubation with the radioactive oligonucleotide. \* indicates the supershifted band; # indicates NF- $\kappa$ B-DNA binding. A representative blot from 3 separate experiments is shown. See Figure 1 for other definitions.

antagonist bosentan. JKC-301 (10  $\mu$ M) and BQ-788 (10  $\mu$ M) inhibited ET-1-driven ICAM-1 expression by a mean  $\pm$  SD of  $47 \pm 13\%$  and  $46 \pm 11\%$ , respectively (Figure 1D). Bosentan (10  $\mu$ M) completely abolished ET-1-mediated ICAM-1 expression (to  $0.9 \pm 1.6\%$ ), indicating that either receptor subtype is capable of mediating the response.

**Necessity of NF- $\kappa$ B and MEK activation for ET-1-mediated ICAM-1 expression.** In the presence of PG490, ET-1-induced increases in mRNA were not detected (Figure 2A), and increased protein expression was strongly inhibited (Figure 2B). To confirm the involvement of NF- $\kappa$ B, an EMSA using a consensus NF- $\kappa$ B sequence was performed, and ET-1 was found to stimulate NF- $\kappa$ B binding in a time-dependent manner (corroborated by supershift indicating the presence of p65 and p50) (Figure 2C). The MEK inhibitor U0126 (10  $\mu$ M) reduced ET-1-induced ICAM-1 expression in human dermal fibroblasts by a mean  $\pm$  SD of  $35 \pm 9\%$  (Figure 2B). Involvement of MEK was confirmed by the detection, by Western blot analysis, of time-dependent ET-1-induced phosphorylation of p42/p44 MAPK, which was abolished by U0126 (results not shown). Residual ICAM-1 expression after blocking of NF- $\kappa$ B activation with PG490 was abolished by the concomitant addition of U0126 (Figure 2B), suggesting that part of the MEK-dependent signaling is independent of NF- $\kappa$ B activation.

**Involvement of NF- $\kappa$ B, MEK, and PKC $\delta$  activation in IL-1 $\beta$ -mediated ICAM-1 expression.** Preincubation of normal dermal fibroblasts with either the MEK inhibitor PD98059 or the NF- $\kappa$ B inhibitor PG490 reduced IL-1 $\beta$ -induced increases in ICAM-1 protein expression by a mean  $\pm$  SD of  $23 \pm 9\%$  and  $67 \pm 5\%$ , respectively (Figure 3A). This was corroborated by the results of quantitative PCR, showing that either inhibitor inhibited IL-1 $\beta$ -induced changes in ICAM-1 mRNA (Figure 3B). The PKC $\delta$ -specific inhibitor Rottlerin inhibited ICAM-1 protein expression by  $26 \pm 14\%$  (Figure 3C) and abolished the IL-1 $\beta$ -induced increase in ICAM-1 mRNA expression (Figure 3D). Inhibition of PI 3-kinase (50 nM wortmannin), p38 MAPK (5  $\mu$ M SB203580), or PKC (bisindolylmaleimide I at 100 nM or 500 nM) did not significantly inhibit the IL-1 $\beta$  response (data not shown).

**Transcriptional activation of ICAM-1 expression by ET-1 or IL-1 $\beta$ .** The region of the ICAM-1 promoter that is important in ET-1-mediated regulation of the gene was determined using constructs of -659, -504, -454, -246, and -135 bp upstream of the gene TATAA box (Figure 4A). All 5 ICAM-1 constructs were

efficiently transcribed following transient transfection (Figure 4B). ET-1 or IL-1 $\beta$  treatment significantly increased transcriptional activity of the -659-bp, -504-bp, -454-bp, and -246-bp constructs but failed to increase transcription of the -135-bp promoter construct, implicating transcription factor binding in the region -135 bp to -246 bp, including an NF- $\kappa$ B consensus site at -157 bp.

**Regulation of ICAM-1 expression in normal and scleroderma dermal fibroblasts.** The influence of ET-1 and IL-1 $\beta$  on ICAM-1 expression was investigated in normal dermal fibroblasts and scleroderma dermal fibroblasts. Quantitative PCR revealed that both cytokines up-regulated ICAM-1 mRNA expression in normal dermal fibroblasts (Figure 5A), whereas scleroderma dermal fibroblasts responded only to IL-1 $\beta$  (Figure 5B). A similar effect was seen with regard to changes in cell surface protein expression (Figure 5C). IL-1 $\beta$  was consistently more effective in up-regulating ICAM-1 expression compared with ET-1, as indicated by the differences in mRNA levels (Figure 5A) and in fold induction of protein in normal dermal fibroblasts (Figure 5C).

**Involvement of PKC $\epsilon$  activation in ET-1-mediated up-regulation of ICAM-1.** Since the signal transduction pathways utilized by ET-1 and IL-1 $\beta$  in up-regulating ICAM-1 expression appeared to be very similar, we investigated the role of protein kinases in mediating the effects of ET-1 on ICAM-1 activity, in order to elucidate any possible differences that may explain the phenomena depicted in Figure 5. For this we used selective inhibitors (Figure 6A). Inhibition of PI-3 kinase (50 nM wortmannin) or p38 MAPK (5  $\mu$ M SB203580) had no effect on ET-1-mediated ICAM-1 expression. Bisindolylmaleimide I at 100 nM (a dose that selectively inhibits the classic PKC isoforms as indicated by IC<sub>50</sub> values) failed to inhibit the ET-1 response, whereas inhibition of PKC by 500 nM bisindolylmaleimide I reduced ICAM-1 expression by a mean  $\pm$  SD of  $45 \pm 11\%$ , suggesting activation of a novel PKC isoform. However, although it inhibited IL-1 $\beta$ -induced ICAM-1, the PKC $\delta$ -specific inhibitor Rottlerin (6  $\mu$ M) did not inhibit ET-1-induced increases in ICAM-1 mRNA expression (Figure 6B).

The involvement of PKC $\epsilon$  was confirmed by transfection of fibroblasts obtained from normal and PKC $\epsilon$ -knockout mouse embryos (22). The ICAM-1 pSM promoter construct driving luciferase transiently transfected into mouse wild-type fibroblasts showed robust induction by ET-1, which was significantly re-

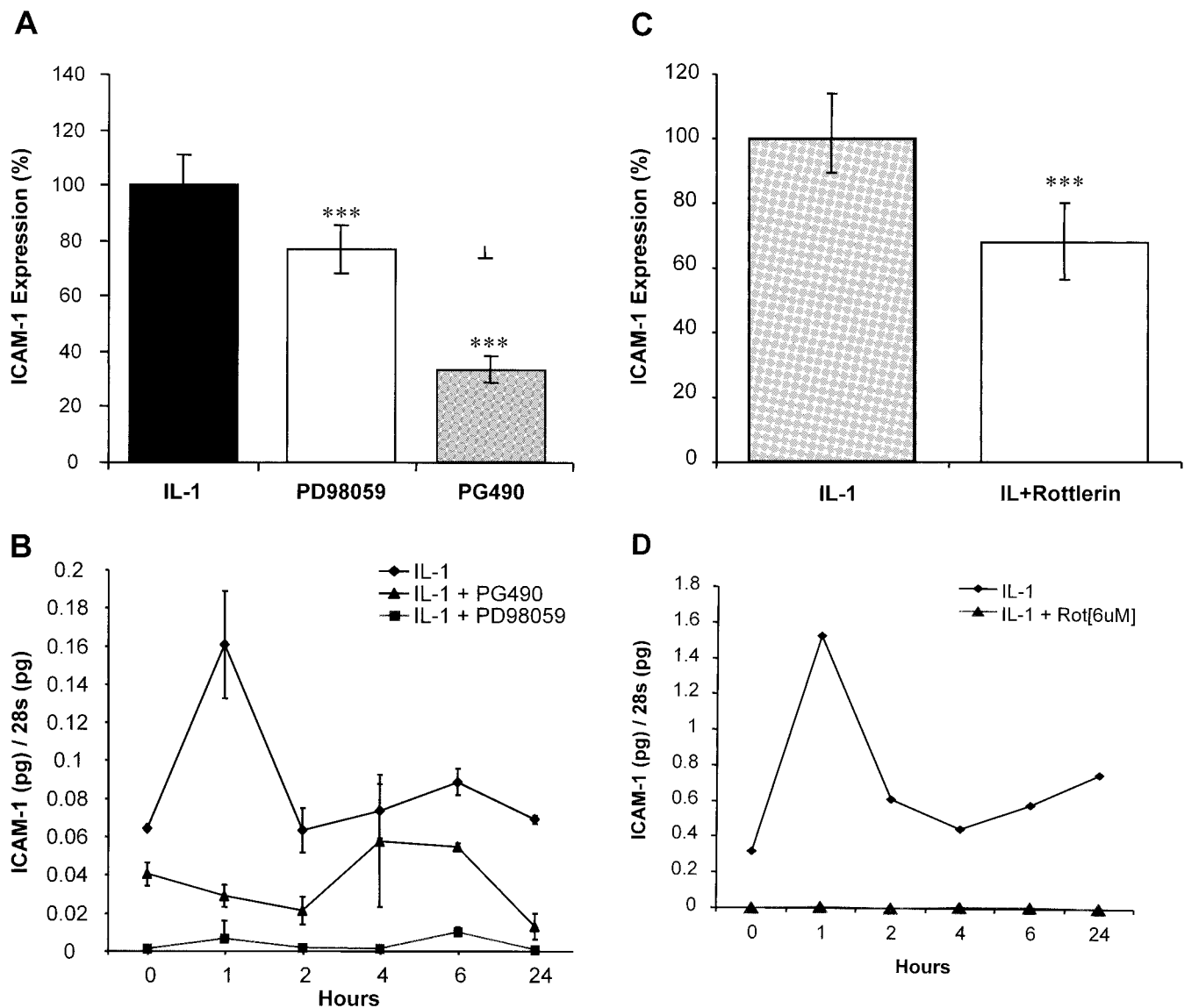


**Figure 3.** Involvement of NF- $\kappa$ B, MEK, and protein kinase C $\delta$  (PKC $\delta$ ) activation in interleukin-1 $\beta$  (IL-1 $\beta$ )-mediated intercellular adhesion molecule 1 (ICAM-1) expression. Fibroblasts were pretreated with the NF- $\kappa$ B inhibitor PG490 (100 nM) or the MEK inhibitor PD98059 (40  $\mu$ M) prior to exposure to IL-1 $\beta$  (10 ng/ml). **A**, Changes in protein expression were detected by cell surface enzyme-linked immunosorbent assay (ELISA). **B**, Messenger RNA isolated from the samples, normalized against 28S ribosomal RNA (rRNA), was used in real-time polymerase chain reaction (PCR) studies for ICAM-1, performed in triplicate. **C** and **D**, Cells were pretreated with the PKC $\delta$ -specific inhibitor Rottlerin (Rot) (6  $\mu$ M) for 1 hour prior to exposure to IL-1 $\beta$  (10 ng/ml). Changes in protein were analyzed by ELISA (**C**), and changes in mRNA, normalized against 28S rRNA, were analyzed by LightCycler PCR, performed in triplicate (**D**). Values are the mean  $\pm$  SD. \*\*\* =  $P < 0.001$  versus IL-1 treatment alone.

duced in transfected PKC $\epsilon$ -knockout mouse fibroblasts (Figure 6C).

Western blotting revealed the presence of PKC $\delta$  and PKC $\epsilon$  in both normal and scleroderma fibroblasts. In scleroderma dermal fibroblasts the expression of PKC $\epsilon$  was not significantly reduced, but the expression of PKC $\delta$  was significantly increased (Figure 6D). Of

note, the ratio of PKC $\epsilon$ :PKC $\delta$  expression was altered from 1:2.1  $\pm$  0.5 (mean  $\pm$  SEM) in normal dermal fibroblasts to 1:4.9  $\pm$  1 in scleroderma dermal fibroblasts.

## DISCUSSION

Our data show that ET-1-induced expression of ICAM-1 on fibroblasts is mediated via both the ET $_A$  and

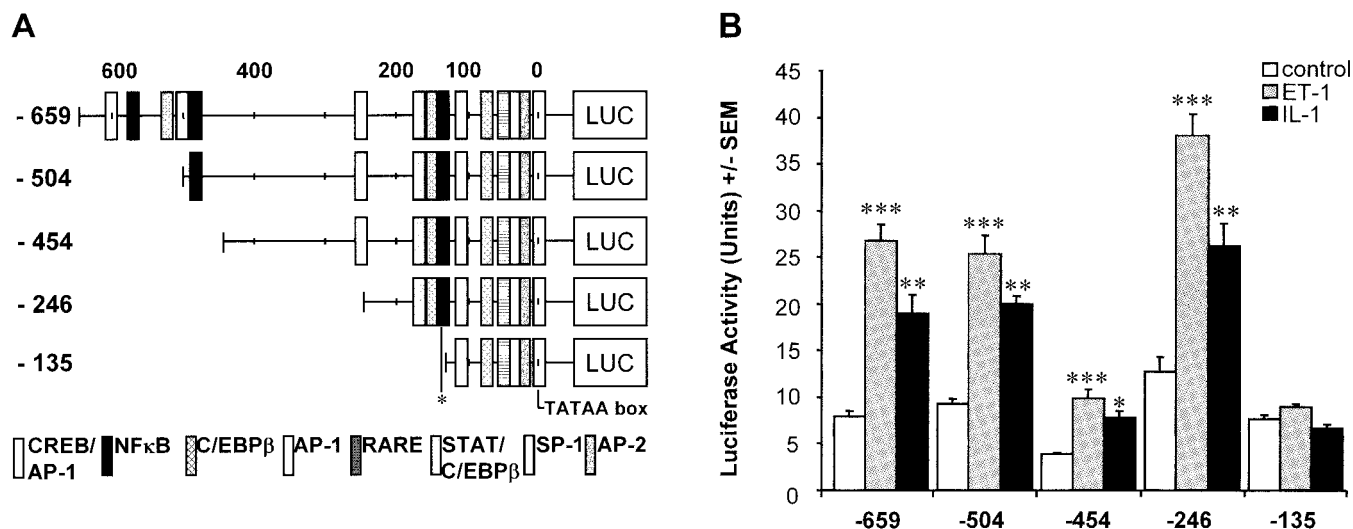


**Figure 4.** Transcriptional activation of ICAM-1 expression by endothelin 1 (ET-1) and IL-1 $\beta$ . **A**, Schematic depiction of 5 deletion constructs of the ICAM-1 promoter (-659, -504, -454, -246, and -135 bp upstream of the transcription start site) driving a firefly luciferase reporter gene. The main transcription factor binding sites contained in each are shown, with the NF- $\kappa$ B site at -157 bp indicated by an asterisk. **B**, The constructs were cotransfected into human dermal fibroblasts with a cytomegalovirus renilla reporter gene. Cells were incubated for 24 hours posttransfection in serum in the presence or absence of ET-1 (100 nM) or IL-1 $\beta$  (10 ng/ml). Values are the mean and SEM from 4 experiments. \* =  $P < 0.05$ ; \*\* =  $P < 0.01$ ; \*\*\* =  $P < 0.001$ , versus control. AP-1 = activator protein 1; c/EBP $\beta$  = CCAAT/enhancer binding protein  $\beta$ ; RARE = retinoic acid response element; STAT = signal transducer and activator of transcription (see Figure 3 for other definitions).

the ET<sub>B</sub> receptor subtypes, consistent with the findings of previous studies of human fibroblast-like synovial cells and rat neonatal cultured cardiac myocytes (8,25), and is abolished only by the dual receptor antagonist bosentan (Figure 1). This indicates that the 2 subtypes must function together to achieve the maximal ET-1 response, which may be due to the existence of endothelin receptor heterodimers (12).

Several transcription factors are known to activate ICAM-1 gene expression, including NF- $\kappa$ B, early growth response protein 1, AP-1, and Ets family members (19). In human dermal fibroblasts the activation of NF- $\kappa$ B appears critical to ET-1-mediated ICAM-1 expression, as shown by the marked inhibition of ET-1-mediated mRNA and protein expression by the NF- $\kappa$ B inhibitor PG490 (Figure 2). The combination of either selective ET receptor antagonist with PG490 did not further inhibit the ET-1 response (data not shown), indicating that activation of either receptor leads to NF- $\kappa$ B activation. Although p42/p44 MAPK activates NF- $\kappa$ B, blocking of MEK activation with U0126 only partially inhibited ICAM-1 up-regulation, and treatment with a combination of MEK and NF- $\kappa$ B inhibitors further inhibited ICAM-1 expression compared with that observed after treatment with either inhibitor alone

(Figure 2B), suggesting some MEK-independent activation of NF- $\kappa$ B.

The signal transduction pathways involved in IL-1 $\beta$ -mediated ICAM-1 expression have been investigated in other cell types, and our data implicating activation of both NF- $\kappa$ B and MEK (Figure 3) are consistent with previously published reports (19). In addition, however, we report the novel finding that PKC $\delta$  has a role in regulating the IL-1 $\beta$  response. Whether PKC $\delta$  functions as part of the signaling cascade is unclear, since to date it has not been reported to fulfill such a role. It is more likely to play a part posttranscriptionally, since IL-1 $\beta$  activation of PKC $\delta$  has been shown to stabilize mRNA (26).

Analysis of the ICAM-1 promoter using a series of ICAM-1 promoter deletion constructs (Figure 4B) demonstrated that ET-1 and IL-1 $\beta$  utilize the same promoter region: -135 to -246 bp. IL-1 $\beta$  has previously been shown to utilize an NF- $\kappa$ B site, with synergistic activation of a neighboring c/EBP $\beta$  site, within this region in astrocytes and endothelium (19), and here we have extended this observation to include dermal fibroblasts. Mapping of this region of the promoter in silico using TESS software (27) revealed that it contains potential binding sites for AP-2, SP-1, RXR/RAR, AP-1,

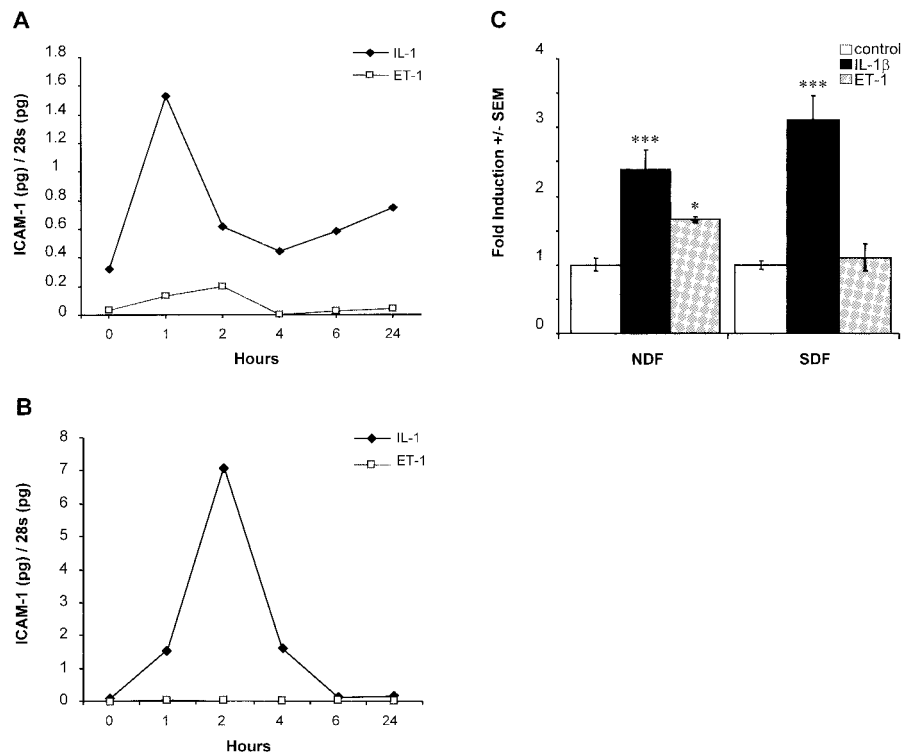


**Figure 5.** Regulation of ICAM-1 expression in normal and scleroderma dermal fibroblasts. **A**, Normal dermal fibroblasts (NDF) and **B**, scleroderma dermal fibroblasts (SDF) were stimulated with IL-1 $\beta$  (10 ng/ml) or endothelin 1 (ET-1) (100 nM) for increasing periods of time, and mRNA isolated from the samples, normalized against 28S rRNA, was used in real-time PCR studies for ICAM-1, performed in triplicate. Values are the mean. **C**, Normal dermal fibroblasts and scleroderma dermal fibroblasts were exposed to IL-1 $\beta$  (10 ng/ml) or ET-1 (100 nM) for 24 hours, and changes in protein expression were analyzed by ELISA. Values are the fold induction over control unstimulated cells (mean  $\pm$  SEM from 4 experiments). \* =  $P < 0.05$ ; \*\*\* =  $P < 0.001$ , versus control. See Figure 3 for other definitions.

and Adf-1, as well as the *c/EBP $\beta$*  and NF- $\kappa$ B sites. Having identified the importance of NF- $\kappa$ B in ET-1-induced ICAM-1 expression, we conclude from these transfection results that binding to the same consensus NF- $\kappa$ B site at -157 bp occurs. ERK-1/2 can also phosphorylate *c/EBP $\beta$*  (28,29), making it likely that ET-1 exposure leads to a pattern of transcription factor binding similar to that induced by IL-1 $\beta$ .

A fraction of ET-1-induced NF- $\kappa$ B activation is MEK-independent. Coupling of the G $\alpha$ s subunit to the ET receptor can lead to an increase in reactive oxygen species (ROS), second messengers that have been shown to activate NF- $\kappa$ B (30), yet we were unable to detect generation of ROS in response to ET-1 in these cells (results not shown).

Coupling of ET-1 receptors to G $\alpha$ q could lead to activation of phospholipase C and hence PKC (8,31,32). The results of PKC inhibition experiments using bisindolylmaleimide I suggested involvement of a novel PKC

subtype (Figure 6A), and the lack of effect of Rottlerin highlighted a possible role of PKC $\epsilon$  (Figure 6B). This was confirmed in studies using PKC $\epsilon$ -knockout mouse fibroblasts (Figure 6C). Activation of PKC $\epsilon$  can lead to the phosphorylation of downstream targets such as MEK (33), as confirmed by our observation of the effect of MEK inhibition and by the rapid and transient increase in p42/p44 MAPK phosphorylation upon addition of ET-1 in Western blot studies (results not shown). This extends our previous findings implicating ET-1-mediated MEK activation in fibroblasts in the regulation of extracellular matrix proteins (23).

ICAM-1 expression in response to IL-1 $\beta$  appears to be increased in scleroderma fibroblasts, but the responses to ET-1 are diminished (Figure 5). This observation is consistent with our previous findings that both mitogenesis and collagen production in scleroderma fibroblasts are reduced in response to ET-1 but intact or enhanced in response to IL-1 $\beta$  (2,3,23), despite

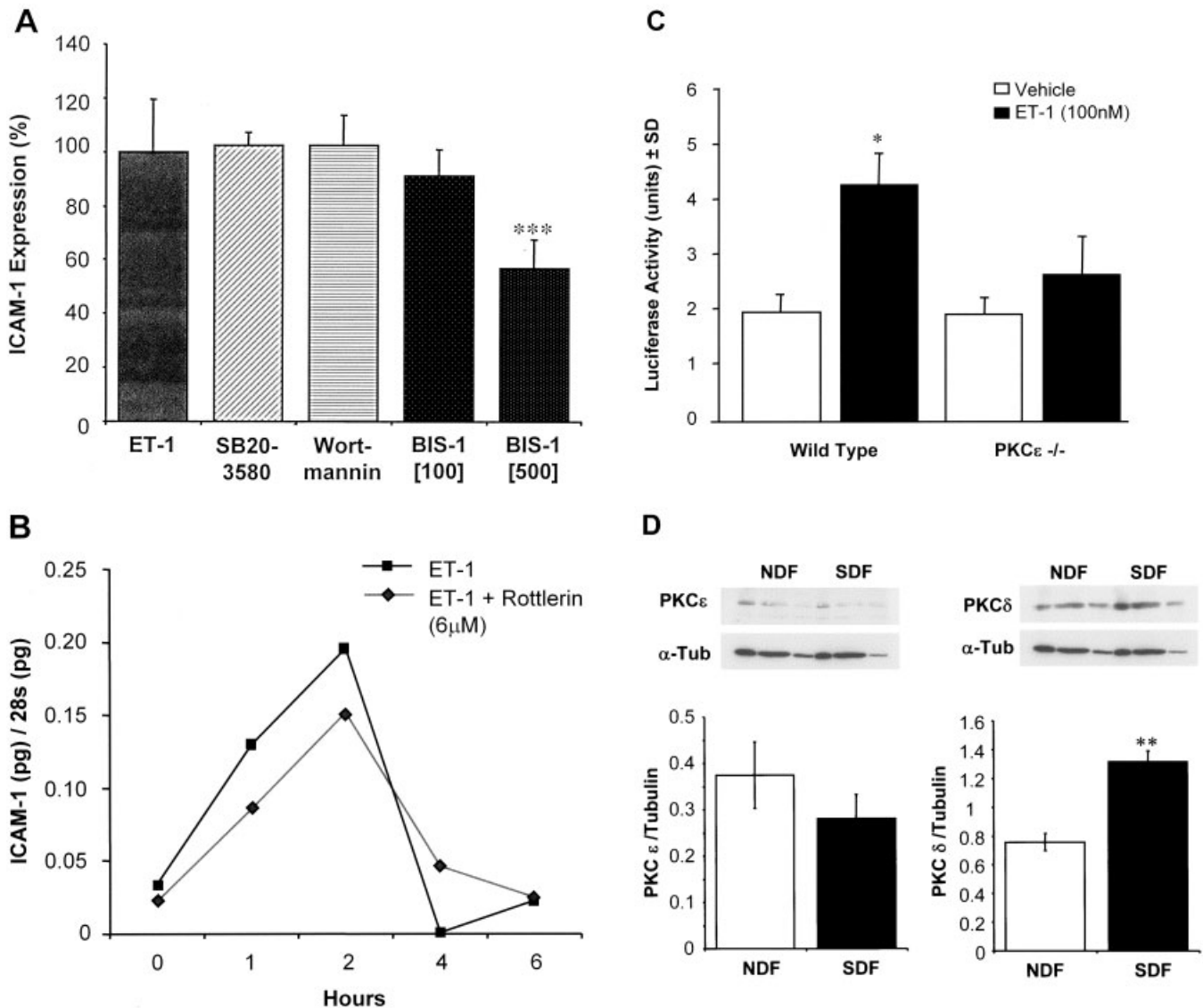


**Figure 6.** Involvement of PKC $\epsilon$  activation in endothelin 1 (ET-1)-mediated up-regulation of ICAM-1. **A**, Cells were pretreated with inhibitors of phosphatidylinositol 3-kinase (50 nM wortmannin), p38 MAPK (5  $\mu$ M SB203580), or PKC (bisindolylmaleimide I [BIS-1]) prior to 24-hour stimulation with ET-1 (100 nM). Values are the percent ICAM-1 expression versus ET-1 stimulation alone (mean and SD from 8 experiments). \*\*\* =  $P < 0.001$  versus ET-1 alone. **B**, Cells were pretreated with the PKC $\delta$ -specific inhibitor Rottlerin (6  $\mu$ M) prior to stimulation with ET-1 (100 nM). Messenger RNA isolated from the samples, normalized against 28S rRNA, was used in real-time PCR studies for ICAM-1, performed in triplicate. Values are the mean. **C**, Fibroblasts from wild-type and PKC $\epsilon$ <sup>-/-</sup> mice were transiently transfected with the ICAM-1 pSM promoter construct and stimulated with ET-1 for 48 hours. \* =  $P < 0.05$  versus vehicle-treated mice. **D**, Whole cell lysate from 3 different unstimulated normal dermal fibroblast (NDF) and scleroderma dermal fibroblast (SDF) strains were subjected to immunoblotting using PKC $\delta$  and PKC $\epsilon$  antibodies. Anti- $\alpha$ -tubulin ( $\alpha$ -tub) was used as a loading control. Mean  $\pm$  SEM PKC:tubulin ratios are shown below the blots. \*\* =  $P < 0.01$  versus normal dermal fibroblasts. See Figure 3 for other definitions.

the close similarity of the pathways regulating ICAM-1 expression in response to ET-1 and IL-1 $\beta$ . Differential activation of the novel PKC isoforms, PKC $\delta$  and PKC $\epsilon$ , by IL-1 $\beta$  and ET-1, respectively, provides a possible explanation for the altered sensitivity of scleroderma

fibroblasts to these 2 cytokines. The ratio of expression of these 2 isoforms differs substantially in scleroderma dermal fibroblasts, with greater PKC $\delta$  expression (Figure 6D). Reduced expression of PKC $\epsilon$  in scleroderma lung fibroblasts has been reported previously (34,35).

There are also reports that ET<sub>A</sub> expression is decreased in scleroderma dermal fibroblasts, while IL-1 receptor expression is increased (3,36,37).

In summary, our data show that ICAM-1 expression in normal dermal fibroblasts in response to ET-1 is dependent on activation of gene transcription by NF- $\kappa$ B binding to the same promoter site used by IL-1 $\beta$ . Activation of both ET<sub>A</sub> and ET<sub>B</sub> receptors is required for maximal ICAM-1 expression, although the signaling cascade leading to NF- $\kappa$ B activation from either receptor appears to be the same. NF- $\kappa$ B activation is due in part to a cascade involving PKC $\epsilon$  and MEK, but also occurs in part via a separate pathway. Activation of MEK additionally leads to NF- $\kappa$ B-independent enhancement of ICAM-1 expression by activating other transcription factors such as c/EBP $\beta$ , AP-1, and SP-1. IL-1 $\beta$  induction of ICAM-1 expression in these cells similarly requires activation of NF- $\kappa$ B and MEK but, unlike ET-1-induced expression, involves PKC $\delta$  activation. We conclude that alterations in ligand sensitivity observed in scleroderma fibroblasts may be due to altered expression of the PKC isoforms involved in the 2 signal cascades, combined with changes in receptor expression.

#### ACKNOWLEDGMENT

We would like to thank Dr. Peter Parker (Cancer Research UK) for donation of the PKC $\epsilon$ <sup>-/-</sup> mouse cells.

#### REFERENCES

- Brain SD, Tippins JR, Williams TJ. Endothelin induces potent microvascular constriction. *Br J Pharmacol* 1988;95:1005-7.
- Shi-Wen X, Denton CP, Dashwood MR, Holmes AM, Bou-Gharios G, Pearson JD, et al. Fibroblast matrix gene expression and connective tissue remodeling: role of endothelin-1. *J Invest Dermatol* 2001;116:417-25.
- Xu S, Denton CP, Holmes A, Dashwood MR, Abraham DJ, Black CM. Endothelins: effect on matrix biosynthesis and proliferation in normal and scleroderma fibroblasts. *J Cardiovasc Pharmacol* 1998;31 Suppl 1:S360-3.
- Mayes MD. Endothelin and endothelin receptor antagonists in systemic rheumatic disease [review]. *Arthritis Rheum* 2003;48:1190-9.
- Hultner L, Ehrenreich H. Mast cells and endothelin-1: a life-saving biological liaison? *Trends Immunol* 2005;26:235-8.
- Lopez Farre A, Riesco A, Espinosa G, Digiuni E, Cernadas MR, Alvarez V, et al. Effect of endothelin-1 on neutrophil adhesion to endothelial cells and perfused heart. *Circulation* 1993;88:1166-71.
- Cunningham ME, Huribal M, Bala RJ, McMillen MA. Endothelin-1 and endothelin-4 stimulate monocyte production of cytokines. *Crit Care Med* 1997;25:958-64.
- Hayasaki Y, Nakajima M, Kitano Y, Iwasaki T, Shimamura T, Iwaki K. ICAM-1 expression on cardiac myocytes and aortic endothelial cells via their specific endothelin receptor subtype. *Biochem Biophys Res Commun* 1996;229:817-24.
- Stratton RJ, Coghlan JG, Pearson JD, Burns A, Sweny P, Abraham DJ, et al. Different patterns of endothelial cell activation in renal and pulmonary vascular disease in scleroderma. *Q J Med* 1998;91:561-6.
- Xu SW, Denton CP, Dashwood MR, Abraham DJ, Black CM. Endothelin-1 regulation of intercellular adhesion molecule-1 expression in normal and scleroderma fibroblasts. *J Cardiovasc Pharmacol* 1998;31 Suppl 1:S545-7.
- Xuan YT, Wang OL, Whorton AR. Regulation of endothelin-induced Ca<sup>2+</sup> mobilization in smooth muscle cells by protein kinase C. *Am J Physiol* 1994;266:C1560-7.
- Gregan B, Schaefer M, Rosenthal W, Oksche A. Fluorescence resonance energy transfer analysis reveals the existence of endothelin-A and endothelin-B receptor homodimers. *J Cardiovasc Pharmacol* 2004;44:S30-3.
- Junneauux C, Mallat A, Serradeil-le Gal C, Goldsmith P, Hanoune J, Lotersztajn S. Coupling of endothelin B receptors to the calcium pump and phospholipase C via Gs and Gq in rat liver. *J Biol Chem* 1994;269:1845-51.
- Doi T, Sugimoto H, Arimoto I, Hiroaki Y, Fujiyoshi Y. Interactions of endothelin receptor subtypes A and B with Gi, Go, and Gq in reconstituted phospholipid vesicles. *Biochemistry* 1999;38:3090-9.
- Shraga-Levine Z, Sokolovsky M. Functional coupling of G proteins to endothelin receptors is ligand and receptor subtype specific. *Cell Mol Neurobiol* 2000;20:305-17.
- Shrikant P, Chung IY, Ballestas ME, Benveniste EN. Regulation of intercellular adhesion molecule-1 gene expression by tumor necrosis factor- $\alpha$ , interleukin-1 $\beta$ , and interferon- $\gamma$  in astrocytes. *J Neuroimmunol* 1994;51:209-20.
- Van de Stolpe A, van der Saag PT. Intercellular adhesion molecule-1. *J Mol Med* 1996;74:13-33.
- Wertheimer SJ, Myers CL, Wallace RW, Parks TP. Intercellular adhesion molecule-1 gene expression in human endothelial cells: differential regulation by tumor necrosis factor- $\alpha$  and phorbol myristate acetate. *J Biol Chem* 1992;267:12030-5.
- Roebuck KA, Finnegan A. Regulation of intercellular adhesion molecule-1 (CD54) gene expression. *J Leukoc Biol* 1999;66:876-88.
- LeRoy EC, Black C, Fleischmajer R, Jablonska S, Krieg T, Medsger TA Jr, et al. Scleroderma (systemic sclerosis): classification, subsets and pathogenesis. *J Rheumatol* 1988;15:202-5.
- Shi-Wen X, Panesar M, Vancheeswaran R, Mason J, Haskard D, Black C, et al. Expression and shedding of intercellular adhesion molecule 1 and lymphocyte function-associated antigen 3 by normal and scleroderma fibroblasts: effects of interferon- $\gamma$ , tumor necrosis factor  $\alpha$ , and estrogen. *Arthritis Rheum* 1994;37:1689-97.
- Castrillo A, Pennington DJ, Otto F, Parker PJ, Owen MJ, Bosca L. Protein kinase C $\epsilon$  is required for macrophage activation and defense against bacterial infection. *J Exp Med* 2001;194:1231-42.
- Xu SW, Howat SL, Renzoni EA, Holmes A, Pearson JD, Dashwood MR, et al. Endothelin-1 induces expression of matrix-associated genes in lung fibroblasts through MEK/ERK. *J Biol Chem* 2004;279:23098-103.
- Cilenti L, Toniato E, Ruggiero P, Fusco C, Farina AR, Tiberio A, et al. Transcriptional modulation of the human intercellular adhesion molecule gene I (ICAM-1) by retinoic acid in melanoma cells. *Exp Cell Res* 1995;218:263-70.
- Schwartzing A, Schlaak J, Lotz J, Pfers I, Meyer zum Buschenfelde KH, Mayet WJ. Endothelin-1 modulates the expression of adhesion molecules on fibroblast-like synovial cells (FLS). *Scand J Rheumatol* 1996;25:246-56.
- Carpenter L, Cordery D, Biden TJ. Protein kinase C $\delta$  activation by interleukin-1 $\beta$  stabilizes inducible nitric-oxide synthase mRNA in pancreatic  $\beta$ -cells. *J Biol Chem* 2001;276:5368-74.
- Schug J, Overton GC. TESS: transcription element search software on the WWW. Technical Report CBIL-TR-1997-1001-v0.0; 1997.

28. Park BH, Qiang L, Farmer SR. Phosphorylation of C/EBP $\beta$  at a consensus extracellular signal-regulated kinase/glycogen synthase kinase 3 site is required for the induction of adiponectin gene expression during the differentiation of mouse fibroblasts into adipocytes. *Mol Cell Biol* 2004;24:8671–80.
29. Qiao L, Han SI, Fang Y, Park JS, Gupta S, Gilfor D, et al. Bile acid regulation of C/EBP $\beta$ , CREB, and c-Jun function, via the extracellular signal-regulated kinase and c-Jun NH2-terminal kinase pathways, modulates the apoptotic response of hepatocytes. *Mol Cell Biol* 2003;23:3052–66.
30. Fubini B, Hubbard A. Reactive oxygen species (ROS) and reactive nitrogen species (RNS) generation by silica in inflammation and fibrosis. *Free Radic Biol Med* 2003;34:1507–16.
31. Robin P, Boulven I, Desmyter C, Harbon S, Leiber D. ET-1 stimulates ERK signaling pathway through sequential activation of PKC and Src in rat myometrial cells. *Am J Physiol Cell Physiol* 2002;283:C251–60.
32. Cramer H, Schmenger K, Heinrich K, Horstmeyer A, Boning H, Breit A, et al. Coupling of endothelin receptors to the ERK/MAP kinase pathway: roles of palmitoylation and G( $\alpha$ )q. *Eur J Biochem* 2001;268:5449–59.
33. Ohashi K, Kanazawa A, Tsukada S, Maeda S. PKC $\epsilon$  induces interleukin-6 expression through the MAPK pathway in 3T3-L1 adipocytes. *Biochem Biophys Res Commun* 2005;327:707–12.
34. Tourkina E, Gooz P, Oates JC, Ludwicka-Bradley A, Silver RM, Hoffman S. Curcumin-induced apoptosis in scleroderma lung fibroblasts: role of protein kinase cepsilon. *Am J Respir Cell Mol Biol* 2004;31:28–35.
35. Tourkina E, Hoffman S, Fenton JW II, Lipsitz S, Silver RM, Ludwicka-Bradley A. Depletion of protein kinase C $\epsilon$  in normal and scleroderma lung fibroblasts has opposite effects on tenascin expression. *Arthritis Rheum* 2001;44:1370–81.
36. Kawaguchi Y, Harigai M, Suzuki K, Hara M, Kobayashi K, Ishizuka T, et al. Interleukin 1 receptor on fibroblasts from systemic sclerosis patients induces excessive functional responses to interleukin 1 $\beta$ . *Biochem Biophys Res Commun* 1993;190:154–61.
37. Kawaguchi Y, Harigai M, Hara M, Suzuki K, Kawakami M, Ishizuka T, et al. Increased interleukin 1 receptor, type I, at messenger RNA and protein level in skin fibroblasts from patients with systemic sclerosis. *Biochem Biophys Res Commun* 1992;184:1504–10.